Letter

Efficient dynamic mixed subgrid-scale model

Prahladh S. Iyer*
Analytical Mechanics Associates, Hampton, Virginia 23666, USA

Mujeeb R. Malik†
NASA Langley Research Center, Hampton, Virginia 23681, USA

(Received 7 March 2024; accepted 30 July 2024; published 3 September 2024)

It is well known that the scale-similarity class of subgrid models have a high correlation with the actual subgrid stresses in *a priori* tests. However, these models are typically underdissipative and not robust enough to be practically useful for large-eddy simulation. On the other hand, the dynamic Smagorinsky model (DSM), which is a popular subgrid model, is sufficiently dissipative and robust, but has a lower correlation with actual subgrid stresses in *a priori* tests. There have been many successful attempts to combine the two models into a "mixed" subgrid model that have typically retained the favorable properties of both. However, most dynamic mixed models require two or more levels of test filtering beyond the (often implicit) grid filtered quantities that are solved, in contrast to a single test filtering operation for the dynamic Smagorinsky model. The additional cost involved in test filtering has likely hindered the widespread use of dynamic mixed models in production codes. We propose an efficient dynamic mixed model that is constrained to have the same subgrid dissipation as the DSM model, and only requires a single level of test filtering. Thus, the additional computational cost is negligible compared to the DSM model. *A posteriori* simulations of the turbulent channel flow reveal that the proposed mixed model is as robust as the DSM model, and more accurate on coarser grids. Notably, smooth-body turbulent separation is better captured by the new model when combined with a standard wall model.

DOI: 10.1103/PhysRevFluids.9.L092601

Many practical flows are turbulent in nature, e.g., those over cars, airplanes, and submarines; predicting its various aspects accurately is a crucial component of the design. Advances in high-performance computing (HPC) are enabling the use of large-eddy simulation (LES) for complex configurations at Reynolds numbers of practical interest. LES subgrid-scale (SGS) modeling has been an active research area for over half a century, starting from the seminal work of Smagorinsky [1], and a number of review papers have summarized the developments in the field [2–4]. Nevertheless, there is still a need for improved SGS models, especially on coarse grid resolutions and varying grid anisotropies.

When the incompressible Navier-Stokes equations are filtered (denoted by $\widetilde{\ }$) by a suitable mathematical definition, we solve for velocity and pressure $(\widetilde{u}_i, \widetilde{p})$, and obtain a closure term for the subgrid stress $(\tau_{ij}^{\mathrm{sgs}})$ that requires modeling:

$$\tau_{ij}^{\mathrm{sgs}} = \widetilde{u_i u_j} - \widetilde{u}_i \widetilde{u}_j. \tag{1}$$

*Contact author: prahladh.s.iyer@ama-inc.com
†Contact author: m.r.malik@nasa.gov

While different definitions and interpretations of the filter are available in literature, $\widetilde{\ }$ is taken to be the (implicit) spatial-grid filter corresponding to the grid size (Δ). Note also that different types of errors due to the filtering operation such as modeling and commutation error are absorbed into this modeling term. Two popular LES SGS models, the dynamic Smagorinsky model (DSM) [5,6] and the scale-similarity model (SSM) [7,8], are shown below:

$$\tau_{ij}^{\mathrm{DSM},d} = -2\nu_{\mathrm{sgs}}^{\mathrm{DSM}}\widetilde{S}_{ij}^{d}, \tag{2}$$

$$\nu_{\mathrm{sgs}}^{\mathrm{DSM}} = c_d\Delta^2|\widetilde{S}|, \quad c_d\Delta^2 = \frac{\langle L_{ij}M_{ij}\rangle}{\langle M_{kl}M_{kl}\rangle}, \quad M_{ij} = 2\big(\widehat{|\widetilde{S}|\widetilde{S}_{ij}^{d}} - \alpha^2|\widehat{\widetilde{S}}|\widehat{\widetilde{S}}_{ij}^{d}\big), \tag{3}$$

$$\tau_{ij}^{\mathrm{SSM}} = L_{ij} = \widehat{\widetilde{u}_i\widetilde{u}}_j - \widehat{\widetilde{u}}_i\widehat{\widetilde{u}}_j. \tag{4}$$

Here, the superscript d denotes the deviatoric part of the tensor, $\widehat{\ }$ denotes test filtering at $\alpha\Delta$, and $\langle\ \rangle$ denotes averaging along homogeneous spatial directions and/or suitable Eulerian/Lagrangian temporal averaging [9]. Note that both models are dynamic in nature due to the dependence on test filtered quantities. The DSM model assumes a linear dependence of $\tau_{ij}^{\mathrm{sgs},d}$ on the resolved strain-rate tensor ($\widetilde{S}_{ij}^{d}$) through a scalar eddy viscosity (ν_{sgs}) that is not accurate in general [8,10,11]. Note that typically $\alpha \approx 2$ for the DSM model [5] and recent versions of the SSM model [8], while $\alpha = 1$ for the original SSM model proposed by Bardina [7]. While the SSM model produces excellent estimation of τ_{ij}^{sgs} in *a priori* tests [7,10], it is insufficiently dissipative to be robust in practical applications. Notably, it underpredicts the subgrid dissipation of the resolved kinetic energy, which is deemed to be an important quantity in LES modeling. On the other hand, the DSM model performs poorly in estimating τ_{ij}^{sgs} in *a priori* tests, but predicts the subgrid dissipation well [3], and consequently is sufficiently robust in practical applications. It is desirable to accurately predict both aspects well, especially on coarser grids and varying grid anisotropies. This has motivated mixed subgrid models of the following form [8,12–15], which generally appear to retain the benefits of both models:

$$\tau_{ij}^{\mathrm{mixed}} = \tau_{ij}^{\mathrm{SSM}} - 2\nu_{\mathrm{sgs}}^{\mathrm{mixed}}\widetilde{S}_{ij}^{d}. \tag{5}$$

While initial attempts used a fixed constant to compute the eddy viscosity, it could make the model overly dissipative; also, dynamic computation of the constant is more accurate for a number of flow phenomena such as transitional regions and for near-wall damping, among others. The Germano identity procedure [5,16] is widely used to dynamically compute constants for LES models, and notably it increases the number of test filtering operations required by one (or more) compared to the baseline model form. The DSM model [Eq. (2)] for instance, explicitly depends only on $\widetilde{\ }$, but the Germano procedure for computing c_d requires one additional level of test filtering ($\widehat{\ }$). The dynamic mixed models (DMMs) of Zang *et al.* [12] and Liu *et al.* [8] require two levels of test filtering (beyond the baseline grid filter) since the Germano identity procedure is directly used on Eq. (5) which already has one level of test filtering due to the τ_{ij}^{SSM} term. Vreman *et al.* [13] suggested that the DMMs be modified to have three levels of test filtering to be more mathematically consistent. The test filtering operation adds significant computational cost for parallel production codes due to the additional communication cost involved (more so on modern computing hardware such as GPUs), and hence it is desirable to minimize such operations in the SGS model for efficiency purposes. Our proposed efficient dynamic mixed model accomplishes this by instantaneously setting the subgrid dissipation of the mixed model to that predicted by the DSM model in lieu of the Germano identity procedure on Eq. (5). Note that one could obtain an efficient model by replacing the SSM model with Clark's gradient model [10] as done by Vreman [17], but that requires the added complexity of defining anisotropic filters [18,19], which may be nontrivial for different unstructured grid topologies. Note that the only required filter-related input for the DSM model (and mixed SSM/DSM model) is the ratio of filter widths (α) as $c_d\Delta^2$ is dynamically computed. The idea of using the subgrid dissipation as a constraint is not entirely new [20–23], although, to the best of the authors' knowledge, it has not been done for the dynamic mixed model to produce an efficient model

with a single level of test filtering with the same communication cost as the SSM or DSM models. The proposed model also explicitly accounts for the subgrid dissipation provided by the SSM model, which may be sufficient on finer grids, thus requiring a negligible eddy-viscosity contribution for stabilization (see fine grid channel wall-resolved LES results for instance). Our proposed model taking $\tau_{ij}^{\mathrm{SSM}} = L_{ij}$ is given below:

$$\tau_{ij}^{\mathrm{mixed}}\widetilde{S}_{ij}^{d} \approx \tau_{ij}^{\mathrm{DSM},d}\widetilde{S}_{ij}^{d}, \tag{6}$$

$$\nu_{\mathrm{sgs}}^{\mathrm{mixed}} = \nu_{\mathrm{sgs}}^{\mathrm{DSM}} + \frac{1}{2}\frac{L_{ij}\widetilde{S}_{ij}^{d}}{\widetilde{S}_{kl}^{d}\widetilde{S}_{kl}^{d}}. \tag{7}$$

While it may be desirable to use Eq. (7) directly, in practice, we regularize the numerator and denominator of the right-hand side term by suitable averaging ($\langle\ \rangle$) and we clip negative values of $\nu_{\mathrm{sgs}}^{\mathrm{mixed}}$ for numerical stability, both of which are analogous to what is done for the DSM model. Thus, the final model reads as follows:

$$\tau_{ij}^{\mathrm{mixed}} = L_{ij} - 2\nu_{\mathrm{sgs}}^{\mathrm{mixed}}\widetilde{S}_{ij}^{d}, \tag{8}$$

$$\nu_{\mathrm{sgs}}^{\mathrm{mixed}} = \left[\nu_{\mathrm{sgs}}^{\mathrm{DSM}} + \frac{1}{2}\frac{\langle L_{ij}\widetilde{S}_{ij}^{d}\rangle}{\langle\widetilde{S}_{kl}^{d}\widetilde{S}_{kl}^{d}\rangle}\right]_{+}. \tag{9}$$

Here, $[\phi]_{+} = 0.5(\phi + |\phi|)$. Note that instead of modifying ν_{sgs} in Eq. (7), one could instead alter the Smagorinsky coefficient c_{mixed} from the DSM value c_d, although it is not clear whether this would improve the accuracy or robustness. We implicitly assume in Eq. (5) that $\tau_{kk}^{\mathrm{mixed}} = L_{kk}$, but our numerical tests with alternate definitions set to 0 or the Yoshizawa model [24] gave nearly identical results for low Mach number flows as expected. Here, the standard procedure is used to compute $\nu_{\mathrm{sgs}}^{\mathrm{DSM}}$ [Eqs. (2) and (3)]. Extension of the DSM model to the proposed mixed model is fairly straightforward—all the required terms are already used in the DSM model computation. The new model thus acts as a "correction" step with under 5% additional computational cost (which can presumably be optimized further) compared to the DSM model. While the mixed model combines the benefits of both the DSM and SSM models, admittedly, some of the deficiencies of the two models are also likely inherited: *ad hoc* clipping and spatial/temporal regularization of eddy viscosity (from DSM), and poorer *a priori* correlations for a sharp spectral cutoff filter (from SSM).

We evaluate the proposed model using *a posteriori* LES for (i) wall-resolved LES (WRLES) of turbulent channel flow at $\mathrm{Re}_\tau \approx 550$, (ii) wall-modeled LES (WMLES) of turbulent channel flow at $\mathrm{Re}_\tau \approx 2000$, and (iii) WMLES of turbulent smooth-body separation over a smooth Gaussian bump at upstream $\mathrm{Re}_\tau \approx 600$. WMLES test cases are included since practical LES applications would likely involve wall modeling due to prohibitive near-wall grid requirements at high Reynolds numbers. Results from two grid resolutions are shown for each case, and compared to those from the DSM model and available reference high-fidelity data. The CharLES solver[1] is used, which is a compressible, cell-centered, low numerical dissipation, nominally second-order accurate, unstructured grid solver [25]. The explicit third-order Runge-Kutta method is used for time stepping. The solver has been validated for a wide range of LES problems using the DSM model [26]. The ratio of test-to-grid filter is set to $\alpha^2 = 5$ based on the recommendation of Vreman *et al.* [11], and test filtering is performed by averaging values at the nodes (computed by averaging across cells sharing the node). For some of the cases simulated, the solver is numerically unstable in the absence of an SGS model, and hence we report the results using the proposed mixed model and the DSM model. All the results were simulated at a reference Mach number of 0.2 at which compressibility effects are expected to be negligible for the quantities of interest reported. The channel flow simulations were run with a source term in the x-momentum equation (and a corresponding term in the total energy

[1]Cascade Technologies, currently Cadence.

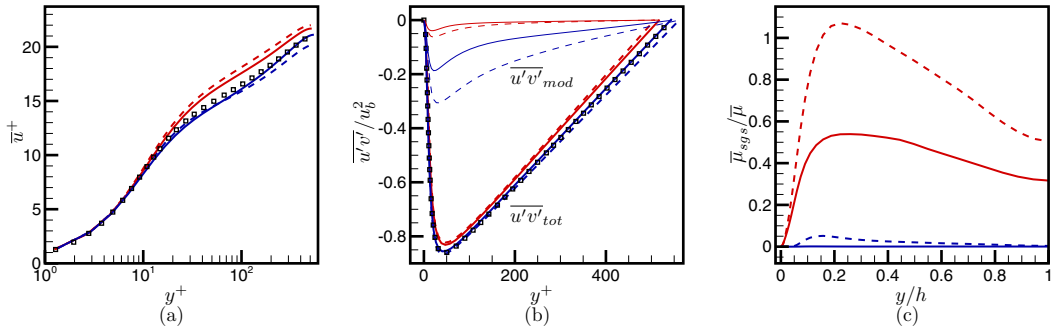

FIG. 1. The variation of time- and spanwise-averaged (a) horizontal velocity ($\overline{u}$), (b) turbulent shear stress ($\overline{u'v'}$), and (c) mean subgrid viscosity ($\overline{\mu}_{\text{sgs}}$) are shown for wall-resolved LES of $\text{Re}_\tau \approx 550$ flow. Legend: (red solid) DSM model, (blue solid) mixed model, and (□) DNS of Lee and Moser [27]. Dashed and solid lines represent coarse and fine grid results, respectively.

equation) computed at each time-stepping stage to maintain a constant reference bulk velocity. Note that averaging along homogeneous directions were used for terms in the SGS models involving $\langle\,\rangle$ and for computing statistics—along x and z for channel flow cases, and z for the bump flow.

WRLES of turbulent channel flow at $\text{Re}_b = \rho_b u_b h/\mu_w = 10\,000$ was performed using a structured hexahedral grid on a domain spanning $L_x, L_y, L_z = 8h, 2h, 3h$, where h is the channel half width, with periodic boundary conditions in the streamwise (x) and spanwise (z) directions. The flow conditions match the DNS of Lee and Moser [27] with an expected $\text{Re}_\tau \approx 550$. The viscous spacings were $\Delta x^+, \Delta y^+, \Delta z^+ = 30, 1.3\text{–}31, 14$, with $N_x, N_y, N_z = 150, 65, 122$ for the fine grid. The coarse grid had $2\times$ spacings in the streamwise and spanwise directions. Results for the DSM and proposed mixed model are shown in Fig. 1. The statistics were averaged over a period of about $15h/u_\tau$. Time- and spatially averaged velocity, turbulent shear stress (modeled and total), and eddy viscosity are shown in the figure. The mixed model yields superior predictions on both grids compared to the DSM model in terms of both velocity and turbulent shear stress. The error in time- and spatially averaged skin-friction prediction [$c_f = \overline{\tau}_w/(0.5\rho_b u_b^2)$] compared to the reference DNS data is -11.3%, $+7.2\%$, -7.6%, and $+1.4\%$ for the coarse DSM, coarse mixed model, fine DSM, and fine mixed model, respectively. The eddy viscosity is much lower for the mixed model compared to the DSM model, and nearly zero for the fine grid (likely due to the resolution chosen), indicating that the majority of the subgrid dissipation is coming from the SSM model term. It is interesting to note that on sufficiently fine grids, the SSM term substantially contributes to the SGS dissipation. Also, notably, the modeled stresses are larger in magnitude (by a factor of 4–6) for the mixed model when compared to the DSM model. The larger modeled stresses for the mixed model suggest that it might be more accurate on coarser grids since it needs to resolve a smaller fraction of the turbulent stresses, although this needs to be thoroughly investigated in the future.

WMLES of turbulent channel flow at $\text{Re}_b = \rho_b u_b h/\mu_w = 43\,500$ was performed using isotropic, uniform, structured hexahedral grids on a domain spanning $L_x, L_y, L_z = 2\pi h, 2h, \pi h$, where h is the channel half width, with periodic boundary conditions in the streamwise (x) and spanwise (z) directions. The flow conditions match the DNS of Lee and Moser [27] with an expected $\text{Re}_\tau \approx 2000$. The viscous spacings were $\Delta_i^+ = 100$ (200), with 20 (10) points per channel half width for the fine (coarse) grid. The equilibrium wall model [28] was used with an exchange location of $0.2h$ for both grids. The statistics were averaged over a period of about $30h/u_\tau$. Time- and spatially averaged velocity, turbulent shear stress (modeled and total), and eddy viscosity are shown in Fig. 2 comparing results using the DSM and mixed models. Both models yield accurate velocity predictions between $y/h \approx 0.1$ and 0.5, with near-wall errors dominating for the DSM model and larger errors in the outer layer for the mixed model. Both models accurately predict the total turbulent shear stress, with the mixed model being marginally more accurate closer to the wall. Here

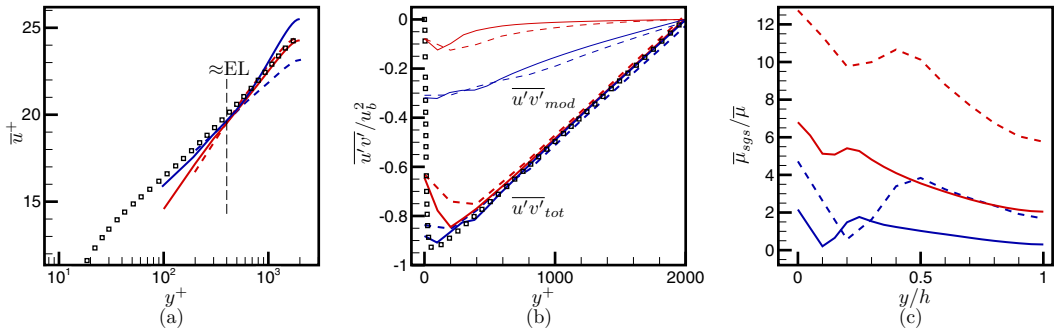

FIG. 2. The variation of time- and spanwise-averaged (a) horizontal velocity ($\overline{u}$), (b) turbulent shear stress ($\overline{u'v'}$), and (c) mean subgrid viscosity ($\overline{\mu}_{\rm sgs}$) are shown for wall-modeled LES of $\mathrm{Re}_\tau \approx 2000$ flow. Legend: (red solid) DSM model, (blue solid) mixed model, and □ DNS of Lee and Moser [27]. Dashed and solid lines represent coarse and fine grid results, respectively. EL refers to the exchange location at which data were input to the wall model.

again, the modeled stresses are larger in magnitude (by ≈3 times) for the mixed model. The error in time- and spatially averaged skin-friction prediction [$c_f = \overline{\tau}_w/(0.5\rho_b u_b^2)$] compared to the reference DNS data is +0.5%, +5.2%, +2.9%, and −2.9% for the coarse DSM, coarse mixed model, fine DSM, and fine mixed model, respectively. The eddy viscosity is again lower for the mixed model compared to the DSM model, but larger in magnitude compared to the WRLES case that had a finer grid resolution in terms of viscous units. Overall, both models yield good predictions for this case. While isotropic grids were used here, it might be interesting to examine the performance of the SGS models on anisotropic grids, and assess any potential benefits of the mixed model in such situations.

WMLES of turbulent smooth-body separation over a Gaussian-shaped bump was simulated at $\mathrm{Re}_L = \rho_\infty u_\infty L/\mu_\infty = 2$ million, where L is the length of the bump, and the Mach number $M_\infty = u_\infty/a_\infty = 0.2$. The shape of the bump is given by $y(x) = h_0 \exp(-(x/x_0)^2)$, with $h_0 = 0.085L$ and $x_0 = 0.195L$. Past studies have indicated that the subgrid model has a dominant effect on the predictions for this flow configuration [29–31], thus making it a useful case for assessing subgrid models. The configuration setup matches the DNS of Uzun and Malik [32]. The top wall is at $y/L = 1$ where freestream boundary conditions are imposed, the inflow plane is at $x/L = -0.67$ where synthetic turbulence inflow boundary conditions are imposed using averaged velocity and turbulent stresses from DNS, and the outflow is at $x/L = 2$. The grid is extruded along the span with a constant spacing, with periodic boundary conditions imposed. Table I lists the grid spacings used for the fine grid along with those used in the DNS. Note that this grid has about 20 and 30–40 points within the boundary layer thickness at $x/L = -0.6$ and 0, respectively. It also has about 10 points within the internal layer at $x/L = 0$. The grid was designed based on insights from past studies [29,33,34]. Snapshots of the grid in the x-y plane are shown in Fig. 3. Note that the grid is isotropic in this plane, and the grid spacing increases based on the distance from the wall. The coarse grid has 2× spacings in all directions compared to the 20 million cell fine grid, and contains

TABLE I. Grid spacings for the fine grid WMLES (fWMLES) compared to the DNS of Uzun and Malik [32].

	Grid	L_z/L	$\Delta z/L$	$\Delta^+_{\rm wall}$ $(x/L = -0.5)$	$\Delta^+_{\rm wall}$ $(x/L = 0)$
DNS	10.2 billion	0.08	1.1×10^{-4}	3.6, 0.6, 8.5	8, 1, 6
fWMLES	20 million	0.08	5×10^{-4}	38, 19, 38	32, 32, 64

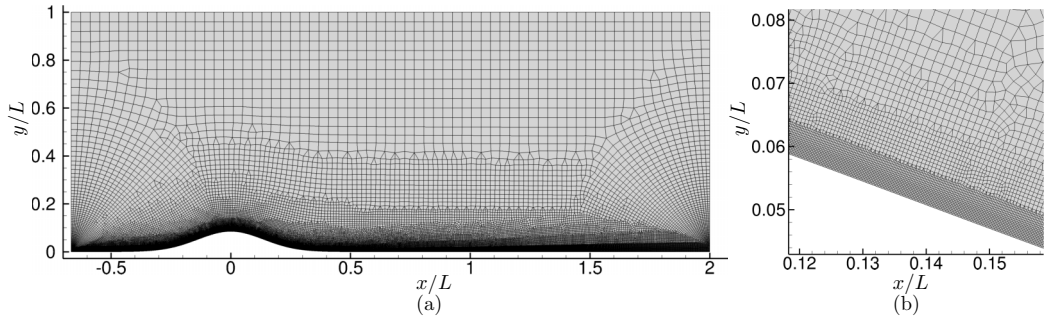

FIG. 3. Snapshots of the grid in a constant spanwise plane (a) over the entire domain, and (b) in the vicinity of separation.

about 6 million points. The equilibrium wall model [28] was used with an exchange location of $5 \times 10^{-4}L$ for all the simulations, which corresponds to the second grid point for the fine grid. The statistics were averaged over a period of about $8L/u_\infty$.

The variation of averaged wall pressure and skin-friction coefficient are shown for both grids, and the DSM and proposed mixed model in Fig. 4. The coarse grid results do not predict sufficient separation for both the SGS models possibly due to the lack of resolving the internal layer and other intricate nonequilibrium dynamics that is responsible for flow separation—the mixed model does marginally better than DSM though. The fine grid mixed model results show excellent agreement with DNS, in contrast to the DSM model which fails to predict any separation at all. These results are generally consistent with the trend of non-eddy-viscosity SGS models performing better for this flow configuration for WMLES [29,30] and WRLES [35]. Note that refining the grid further might place it in a WRLES realm, thus defeating the purpose of using WMLES. It is of interest to point out that the DSM model does predict separation (though it underpredicts the size) on a similar resolution polyhedral grid [29,30,33,34], while a recent study found that the model did not predict any separation even on a much finer (993 million) hexahedral-dominant grid [31] (consistent with the present results), although the reasons for the differences are unclear. Averaged velocity and turbulent shear stress profiles are shown for the fine grid at $x/L = -0.2$, 0, and 0.2, which correspond to favorable, inflectional, and adverse pressure gradient regions in Fig. 5. While the DSM model results are reasonable at $x/L = -0.2$, the mixed model shows substantially improved velocity and stress predictions overall. Some differences between the mixed model results and DNS may be due to the limitations of the equilibrium wall model used here. Overall, the fine grid mixed

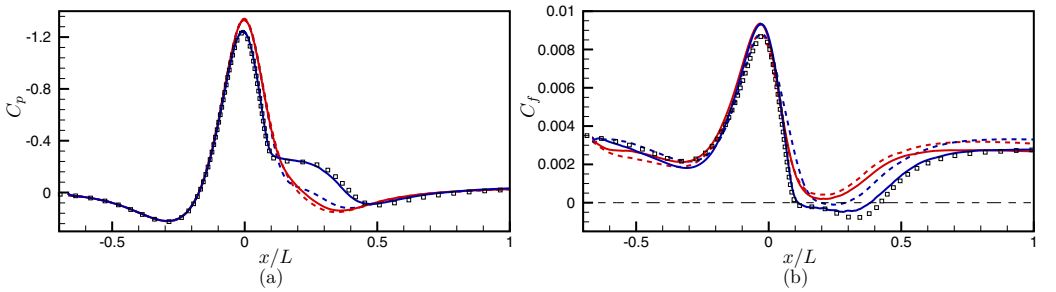

FIG. 4. The variation of time- and spanwise-averaged wall (a) pressure coefficient (C_p) and (b) skin-friction coefficient (C_f) for the speed bump flow. Legend: (red solid) DSM model, (blue solid) mixed model, and (□) DNS of Uzun and Malik [32]. Dashed and solid lines represent coarse and fine grid results, respectively.

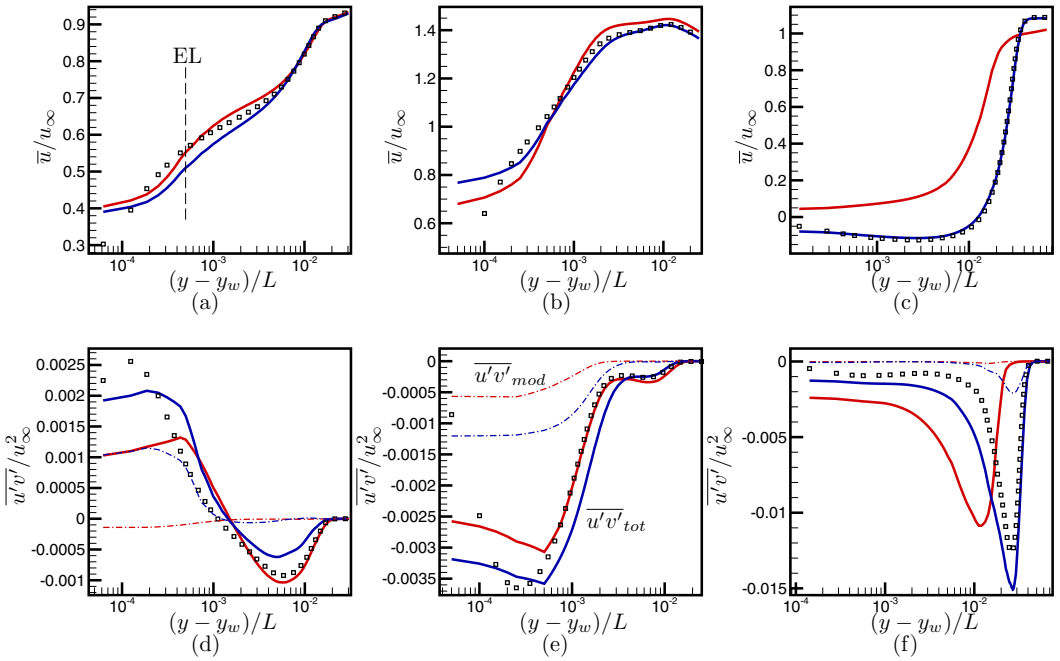

FIG. 5. Profiles of time- and spanwise-averaged (a)–(c) horizontal velocity ($\overline{u}/u_\infty$), and (d)–(f) turbulent shear stress ($\overline{u'v'}/u_\infty^2$) is shown for the speed bump flow at (a), (d) $x/L = -0.2$, (b), (e) $x/L = 0$, and (c), (f) $x/L = 0.2$ for the fine grid. Legend: (red solid) DSM model, (blue solid) mixed model, and (□) DNS of Uzun and Malik [32]. EL refers to the exchange location at which data were input to the wall model.

model WMLES shows excellent agreement with DNS for this complex flow configuration in spite of using a substantially coarser grid (500×).

We proposed an efficient dynamic mixed subgrid model with a single level of test filtering by using an SGS dissipation constraint in lieu of the Germano identity procedure to combine the scale-similarity and dynamic Smagorinsky models. The model was evaluated on wall-resolved LES of a turbulent channel, and wall-modeled LES of a turbulent channel and smooth-body separation using an unstructured solver at two grid levels. The model was robust for all the simulations, and generally gave encouraging and improved predictions compared to the DSM model for the grid resolutions used. Notably, it produced substantially more accurate results for turbulent smooth-body separation, which is a challenging phenomenon to predict. Future work will involve assessing the model on more applications and grid topologies/anisotropies.

This research was sponsored by the NASA Transformational Tools and Technologies (T^3) Project of the Transformative Aeronautics Concepts Program under the Aeronautics Research Mission Directorate. The work of the first author was sponsored by NASA under Contract No. 80LARC23DA003. We thank Cascade Technologies for providing the CharLES solver and consultation in use of the code, and Ponnampalam Balakumar, Dave Lockard, and Gary Coleman for comments on the manuscript.

[1] J. Smagorinsky, General circulation experiments with the primitive equations: I. The basic experiment, Mon. Weather Rev. **91**, 99 (1963).

[2] M. Lesieur and O. Metais, New trends in large-eddy simulations of turbulence, Annu. Rev. Fluid Mech. **28**, 45 (1996).
[3] C. Meneveau and J. Katz, Scale-invariance and turbulence models for large-eddy simulation, Annu. Rev. Fluid Mech. **32**, 1 (2000).
[4] R. D. Moser, S. W. Haering, and G. R. Yalla, Statistical properties of subgrid-scale turbulence models, Annu. Rev. Fluid Mech. **53**, 255 (2021).
[5] M. Germano, U. Piomelli, P. Moin, and W. H. Cabot, A dynamic subgrid-scale eddy viscosity model, Phys. Fluids **3**, 1760 (1991).
[6] D. K. Lilly, A proposed modification of the Germano subgrid-scale closure method, Phys. Fluids **4**, 633 (1992).
[7] J. Bardina, J. Ferziger, and W. Reynolds, Improved subgrid-scale models for large-eddy simulation, *13th Fluid and Plasma Dynamics Conference* (AIAA, Snowmass, CO, USA, 1980), doi:10.2514/6.1980-1357.
[8] S. Liu, C. Meneveau, and J. Katz, On the properties of similarity subgrid-scale models as deduced from measurements in a turbulent jet, J. Fluid Mech. **275**, 83 (1994).
[9] C. Meneveau, T. S. Lund, and W. H. Cabot, A lagrangian dynamic subgrid-scale model of turbulence, J. Fluid Mech. **319**, 353 (1996).
[10] R. A. Clark, J. H. Ferziger, and W. C. Reynolds, Evaluation of subgrid-scale models using an accurately simulated turbulent flow, J. Fluid Mech. **91**, 1 (1979).
[11] B. Vreman, B. Geurts, and H. Kuerten, Large-eddy simulation of the turbulent mixing layer, J. Fluid Mech. **339**, 357 (1997).
[12] Y. Zang, R. L. Street, and J. R. Koseff, A dynamic mixed subgrid-scale model and its application to turbulent recirculating flows, Phys. Fluids **5**, 3186 (1993).
[13] B. Vreman, B. Geurts, and H. Kuerten, On the formulation of the dynamic mixed subgrid-scale model, Phys. Fluids **6**, 4057 (1994).
[14] M. V. Salvetti and S. Banerjee, *A priori* tests of a new dynamic subgrid-scale model for finite-difference large-eddy simulations, Phys. Fluids **7**, 2831 (1995).
[15] K. Horiuti, A new dynamic two-parameter mixed model for large-eddy simulation, Phys. Fluids **9**, 3443 (1997).
[16] M. Germano, Averaging invariance of the turbulent equations and similar subgrid-scale modeling, CTR Manuscript 116 (1990).
[17] B. Vreman, B. Geurts, and H. Kuerten, Large-eddy simulation of the temporal mixing layer using the Clark model, Theor. Comput. Fluid Dyn. **8**, 309 (1996).
[18] H. Kobayashi and Y. Shimomura, Inapplicability of the dynamic Clark model to the large eddy simulation of incompressible turbulent channel flows, Phys. Fluids **15**, L29 (2003).
[19] A. Vreman, Comment on "Inapplicability of the dynamic Clark model to the large eddy simulation of incompressible turbulent channel flows" [Phys. Fluids **15**, L29 (2003)], Phys. Fluids **16**, 490 (2004).
[20] N. Park and K. Mahesh, A velocity-estimation subgrid model constrained by subgrid scale dissipation, J. Comput. Phys. **227**, 4190 (2008).
[21] Y. Shi, Z. Xiao, and S. Chen, Constrained subgrid-scale stress model for large eddy simulation, Phys. Fluids **20**, 011701 (2008).
[22] K. Abe, An improved anisotropy-resolving subgrid-scale model with the aid of a scale-similarity modeling concept, Int. J. Heat Fluid Flow **39**, 42 (2013).
[23] H. Qi, X. Li, R. Hu, and C. Yu, Quasi-dynamic subgrid-scale kinetic energy equation model for large-eddy simulation of compressible flows, J. Fluid Mech. **947**, A22 (2022).
[24] A. Yoshizawa, Statistical theory for compressible turbulent shear flows, with the application to subgrid modeling, Phys. Fluids **29**, 2152 (1986).
[25] G. A. Brès, F. E. Ham, J. W. Nichols, and S. K. Lele, Unstructured large-eddy simulations of supersonic jets, AIAA J. **55**, 1164 (2017).
[26] G. I. Park, Wall-modeled large eddy simulation in an unstructured mesh environment, Ph.D. thesis, Stanford University, 2014.
[27] M. Lee and R. D. Moser, Direct numerical simulation of turbulent channel flow up to $\mathrm{Re}_\tau \approx 5200$, J. Fluid Mech. **774**, 395 (2015).

[28] S. Kawai and J. Larsson, Wall-modeling in large eddy simulation: Length scales, grid resolution, and accuracy, Phys. Fluids **24**, 015105 (2012).

[29] P. S. Iyer and M. R. Malik, Wall-modeled LES of turbulent flow over a two dimensional Gaussian bump, ICCFD11-2022-0204, https://www.iccfd.org/iccfd11/assets/pdf/papers/ICCFD11_Paper-0204.pdf (2022).

[30] R. Agrawal, M. P. Whitmore, K. P. Griffin, S. T. Bose, and P. Moin, Non-Boussinesq subgrid-scale model with dynamic tensorial coefficients, Phys. Rev. Fluids **7**, 074602 (2022).

[31] D. Zhou and H. J. Bae, Sensitivity analysis of wall-modeled large-eddy simulation for separated turbulent flow, J. Comput. Phys. **506**, 112948 (2024).

[32] A. Uzun and M. R. Malik, High-fidelity simulation of turbulent flow past Gaussian bump, AIAA J. **60**, 2130 (2022).

[33] M. P. Whitmore, K. P. Griffin, S. T. Bose, and P. Moin, *Large-Eddy Simulation of a Gaussian Bump with Slip-Wall Boundary Conditions, Annual Research Briefs - 2021*, Center for Turbulence Research (Stanford University, Stanford, CA, 2021).

[34] P. S. Iyer and M. R. Malik, Wall-modeled LES of the three-dimensional speed bump experiment, AIAA (2023), doi:10.2514/6.2023-0253.

[35] A. Uzun and M. R. Malik, A dynamic nonlinear subgrid-scale model for large-eddy simulation of complex turbulent flows, NASA Technical Report No. NASA-TM-20220013891 (2022).